DEPOSITION OF METAL OXIDES (MO-CU-TI-FE) USING THE CATHODIC CAGE DEPOSITION TECHNIQUE

Ediones Maciel de Sousa[1,2], Marcos Cristino de Sousa Brito[3], Lucas Pereira da Silva[3], Brenda Jakellinny de Sousa Nolêto[3], Lauriene Gonçalves da Luz Silva[3], Renan Matos Monção[3], Lucas Santos Garreto[4], Thercio Henrique de Carvalho Costa[5], Samuel Filgueiras Rodrigues[1], Cleânio da Luz Lima[2], Rômulo Ribeiro Magalhães de Sousa[3].

[1]Department of Mechanical Engineering – Federal Institute of Education, Science and Technology of Maranhão (IFMA), São Luís, MA, Brazil.
edionesmaciel.36@gmail.com
samuel.filgueiras@ifma.edu.br
[2]Physics Department – Federal University of Piauí (UFPI), Teresina, PI, Brazil.
edionesmaciel.36@gmail.com
cleanio@ufpi.edu.br
[3]Graduate Program in Materials Science and Engineering – Federal University of Piauí (UFPI), Teresina, PI, Brazil.
marcoscristino@ufpi.edu.br
lucaspereirasilva7600@gmail.com
brendajakellinny@gmail.com
lauriene@ufpi.edu.br
renan.matos@ufpi.edu.br
romulorms@gmail.com
[4]Graduate Program in Materials Science and Technology – Federal Institute of Education, Science and Technology of Maranhão (IFMA), São Luís, MA, Brazil.
lucasgarreto@acad.ifma.edu.br
[5]Department of Mechanical Engineering – Federal University of Rio Grande do Norte (UFRN), Natal, RN, Brazil.
thercioc@ufrn.edu.br

ABSTRACT

This study analysed the formation of metal oxide films (Mo-Cu-Ti-Fe) using the cathodic cage deposition method. By varying the cage cover, films with different properties and compositions were produced. These films were analysed using scanning electron microscopy (SEM), energy dispersive X-ray spectroscopy (EDS), X-ray diffractometry (XRD) and roughness measurements. The results showed that films with good adhesion to the substrate were formed, as well as the presence of crystalline phases typical of the deposited oxides. These characteristics indicate that the cathodic cage deposition method is suitable for producing high-quality thin films, making it a promising alternative for applications in catalysis, sensors and electronic devices.

KEYWORDS: *Cathodic Cage Deposition, Metal Oxides, Thin Films, Molybdenum*

I. INTRODUCTION

Today, the accelerated advancement of technology demands a continuous search for new materials that meet the growing needs of industry. In this context, transition metal oxides, particularly molybdenum oxides, have stood out due to their abundance, ease of processing, and the wide range of properties they exhibit. Research on molybdenum compounds is becoming increasingly relevant. Nitrides and oxides are widely used in surface engineering due to their excellent hardness, corrosion

resistance, low coefficient of friction, and solid lubrication characteristics [1]. Molybdenum oxide can be obtained through a variety of techniques, such as cathodic arc [2], ion beam [3], nitriding of molybdenum films [4], ion implantation [5], plasma-enhanced chemical vapor deposition [5], sol-gel [6], pulsed laser deposition [9], and plasma deposition with cathodic cages at cathodic and floating potentials [7], among other techniques.

On the other hand, TiO_2 films stand out for their unique properties, such as chemical stability, low toxicity, low cost, high refractive index, high permittivity and biocompatibility [8]. It is a metal oxide with excellent dielectric, optical and electronic properties. It crystallizes in three structural phases: anatase, rutile and brookite. The properties of the TiO_2 thin film depend on the proportion of each phase present in the developed film [9]. The anatase phase, in particular, offers advantages that enable the application of TiO_2 thin films in industry, such as anti-corrosion, chemical reactivity and photocatalysis. Additionally, depending on the preparation conditions, the anatase phase exhibits high durability, a high refractive index (n=2.3), high resistivity, and a high dielectric constant – characteristics that are essential, for example, in anti-reflective films and photochemical solar cells [10], [11], [12].

TiO_2 thin films can be synthesized using numerous techniques, such as chemical vapor deposition (CVD) [13], [14], physical vapor deposition (PVD) [15], [16] and reactive sputtering [17].

Copper and copper oxide are gaining popularity in both fundamental science and technological applications. Due to their excellent thermal and electrical conductivity, as well as theiir bioactive properties, copper and its oxides are considered to be of great importance. Copper oxide, a p-type semiconductor, can exist in two forms: copper (I) oxide (Cu_2O, also known as cuprous oxide) and copper (II) oxide (CuO, also known as cupric oxide).

Copper oxide (Cu_2O) films are widely valued in the construction of photovoltaic solar cells and photoelectric cells due to their favorable energy bandgap, low manufacturing cost, and wide availability for production [18]. Various deposition techniques have been used to produce Cu_2O films, including reactive sputtering [19], electrodeposition [20], DC reactive sputtering [21] and thermal oxidation [22].

Iron oxide is a compound that exhibits a range of interesting properties, such as catalytic, optical, magnetic, and semiconducting properties, which vary depending on its structure [23], [24]. Iron oxides, in particular, can exist in different chemical compositions and lattice arrangements, including FeO (wüstite), Fe_3O_4 (magnetite), γ-Fe_2O_3 (maghemite) and α-Fe_2O_3 (hematite). Hematite iron oxide (α-Fe_2O_3) is considered one of the main candidates for photoanode material in photoelectrochemical water-splitting devices [25]. The versatility of iron oxide (Fe_2O_3) is evidenced by the variety of deposition techniques used in its production, including magnetron sputtering [26], pulsed laser deposition (PLD) [27], electrodeposition [28], sol-gel deposition [29], [30] and chemical vapor deposition (CVD) [31]. This diversity makes it possible to obtain films with specific properties for different applications.

This work aims to synthesize and characterize thin films of metal oxides (Mo-Cu-Ti-Fe) using the cathodic cage deposition technique in order to investigate their mechanical properties.

II. EXPERIMENTAL SECTION

2.1. Film deposition

AISI 316 steel, a commercially available material, was used in this study in the form of samples with the following chemical composition (wt%): 0.03% C, 17% Cr, 12% Ni, 2.2% Mo, and Fe (balance).

The samples were machined into a rectangular shape with dimensions of 15×10×3 mm^3. After the machining process, the samples were sanded using water sandpaper of different grain sizes: 220, 400, 600, and 1200 mesh. The samples were then polished on felt discs using alumina, immersed in 70% alcohol and subjected to ultrasonic agitation for 10 minutes. Finally, the samples were dried using a conventional dryer with a hot air flow. The films were deposited using a molybdenum cathode cage with dimensions of 45 mm in height and 90 mm in diameter. This structure features 8 mm diameter

holes, evenly distributed, with a center-to-center distance of 9 mm (Figure 1). The cage lid used in the procedures was made of molybdenum, titanium, steel and copper. Table 1 details the composition of the cage and the parameters used in the treatment.

Table 1 - Treatments parameters.

Sample	Cage		Atmosphere (sccm)	Temperature (°C)	Time (h)
	Cylinder	Lid			
GaMoTaMo	Mo	Mo	50 Ar – 50 O_2	400	5
GaMoTaTi		Ti			
GaMoTaFe		Steel			
GaMoTaCu		Cu			

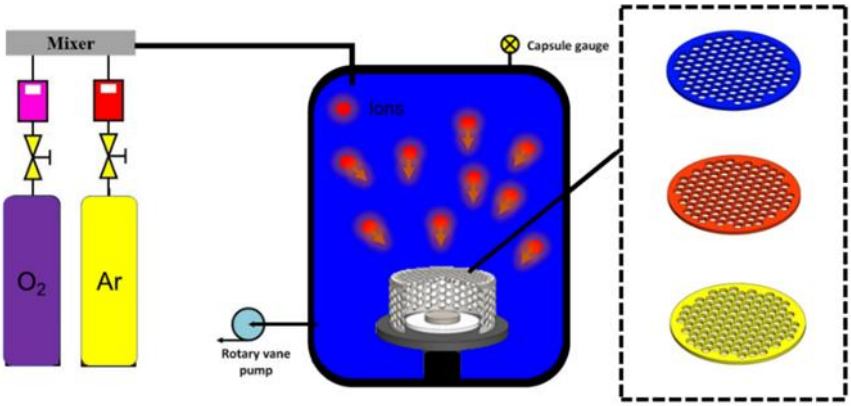

Figure 1 - Schematic illustration of the plasma deposition reactor equipped with a molybdenum cathode cage and Molybdenum, Titanium, Steel and Copper caps.

2.2. Morphological and structural analysis

The samples were characterized by X-ray diffraction (Shimadzu DRX-6000) using Cu-Kα radiation (λ = 1.55406 Å). The copper tube operated with a voltage of 45 kV, a current of 40 mA, and a scanning range of 2θ from 30° to 90°. The Vickers microhardness test (INSIZE model ISH-TDV 1000 A-B) was carried out with a load of 50 gf, resulting in an average value from five measurements. The cross-sectional analysis was performed using scanning electron microscopy (SEM) with an FEI COMPANY QUANTA FEG 250 model. To determine the chemical elements present in the deposited films, the EDS accessory of the SEM was used, with an acceleration voltage of 20 kV. The adhesion test was performed using an INSIZE microdurometer, model ISH-BRV. In this test, an impression was made at the center of the treated sample, applying a load of 1471 N. The roughness test was carried out using a MITUTOYO model SJ-210 portable roughness meter. For this, 5 measurements were taken on each sample, each one starting from the centre to the edge of the sample. The sampling and evaluation lengths (lm) were 0.8 mm and 4.0 mm, respectively.

III. RESULTS AND DISCUSSION

3.1. Morphological, elemental and structural characterization

The morphology and elemental composition of the films were analyzed using SEM and EDS, as shown in Figure 2. The figure reveals the uniform appearance of the samples under all treatment conditions, demonstrating the efficiency of the cathodic cage treatment technique [32]. In Figure 2a, where a Mo cage and lid are used, a layer thickness of approximately 1.78 µm is observed, presenting a significantly denser appearance compared to the cage with a titanium lid (Figure 2b). Despite this, the use of a titanium cage results in a greater layer thickness, approximately 5.16 µm, compared to that obtained with Mo. The samples treated with steel lids (Figure 2c) and copper lids (Figure 2d) exhibit average layer thickness of 0.42 µm and 1.09 µm, respectively. The thickness and density of the deposited films show a variation directly linked to the characteristics of the material that makes up the cage lid, as described by [33]. This phenomenon can be explained using Arrhenius law (Equation

1), which establishes a relationship between the diffusion coefficient (D) and parameters such as temperature (T) and activation energy (Q).

$$D = D_0 exp\left(-\frac{Q}{RT}\right) \qquad Equation\ 1$$

The activation energy of each material plays a decisive role in the mobility of atoms during the deposition process. Materials with different ionisation energy levels result in varying concentrations of active species in the plasma, which directly affects the kinetics of nitride formation [34]. In addition, the choice of film depends on its intended application, considering the different properties of each material. However, when layer thickness is a critical factor, the titanium lid stands out as the best option, due to the difference in activation energy associated with the materials.

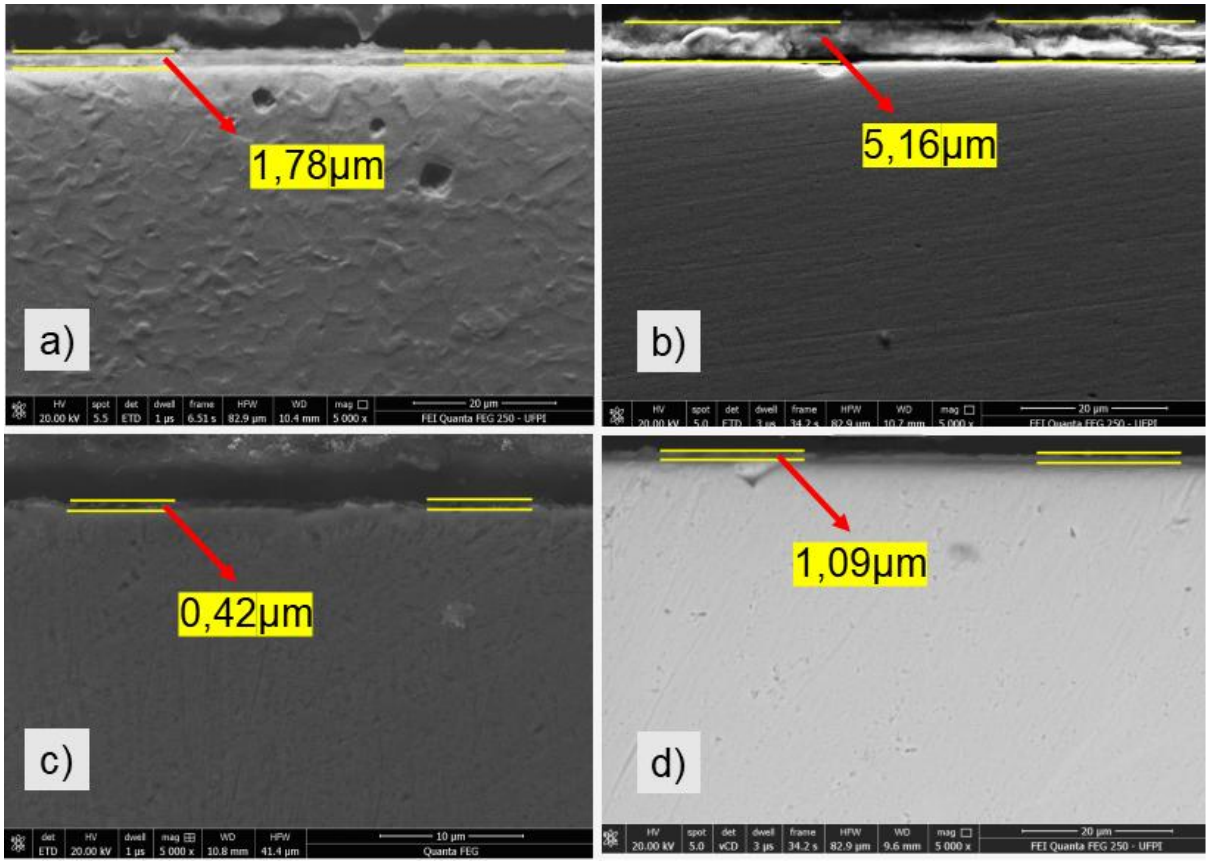

Figure 2 - Scanning electron microscopy (SEM) Molybdenum cage with (a) Molybdenum, (b) Titanium, (c) Steel and (d) Copper lid.

Figure 3 shows the EDS spectra of the plasma-deposited films, highlighting the composition of these materials. The spectral analysis confirms the presence of elements from the atmosphere (oxygen), the body of the molybdenum cage, the lids (molybdenum, titanium, steel, and copper), and the AISI 316 sample (iron, chromium, and nickel). The GaMoTaMo sample exhibits a significant amount of molybdenum, which is directly related to the composition of the cage body and lid. This result is corroborated by X-ray diffractometry (XRD) analysis. In the GaMoTaTi sample, the presence of titanium is attributed to the use of a titanium lid. The GaMoTaFe sample, in turn, shows an increase in iron content due to the stainless steel lid. Similarly, the presence of copper is observed in the GaMoTaCu sample, as a copper lid was used in this case. Finally, the EDS spectra reveal that the molybdenum concentration in the deposition was significantly higher when the cage body and molybdenum lid were used, demonstrating the efficiency of the cathodic cage deposition technique [35].

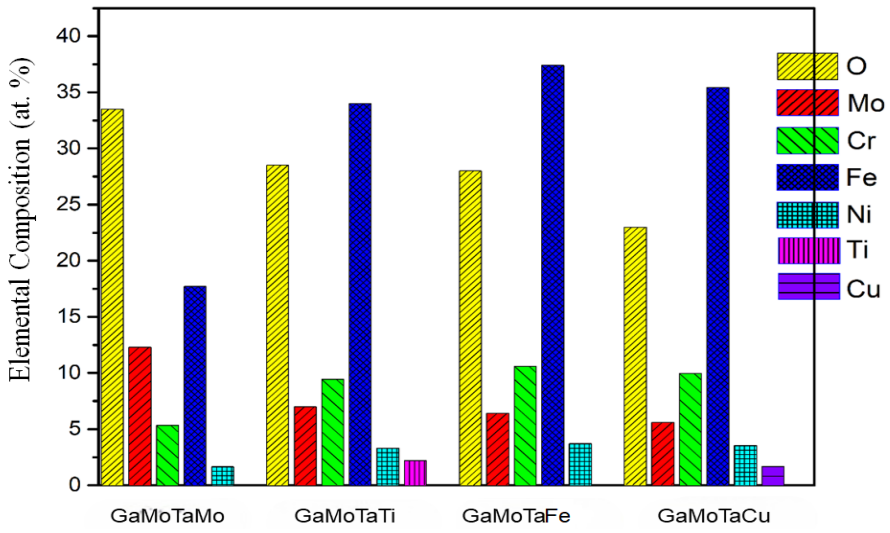

Figure 3 - Energy dispersive X-ray spectroscopy (EDS) Molybdenum cage with Molybdenum (GaMoTaMo), Titanium (GaMoTaTi), Steel (GaMoTaFe) and Copper lid (GaMoTaCu).

Figure 4 shows the X-ray spectra of AISI 316 austenitic stainless steel samples subjected to plasma deposition treatment using the cathodic cage technique.

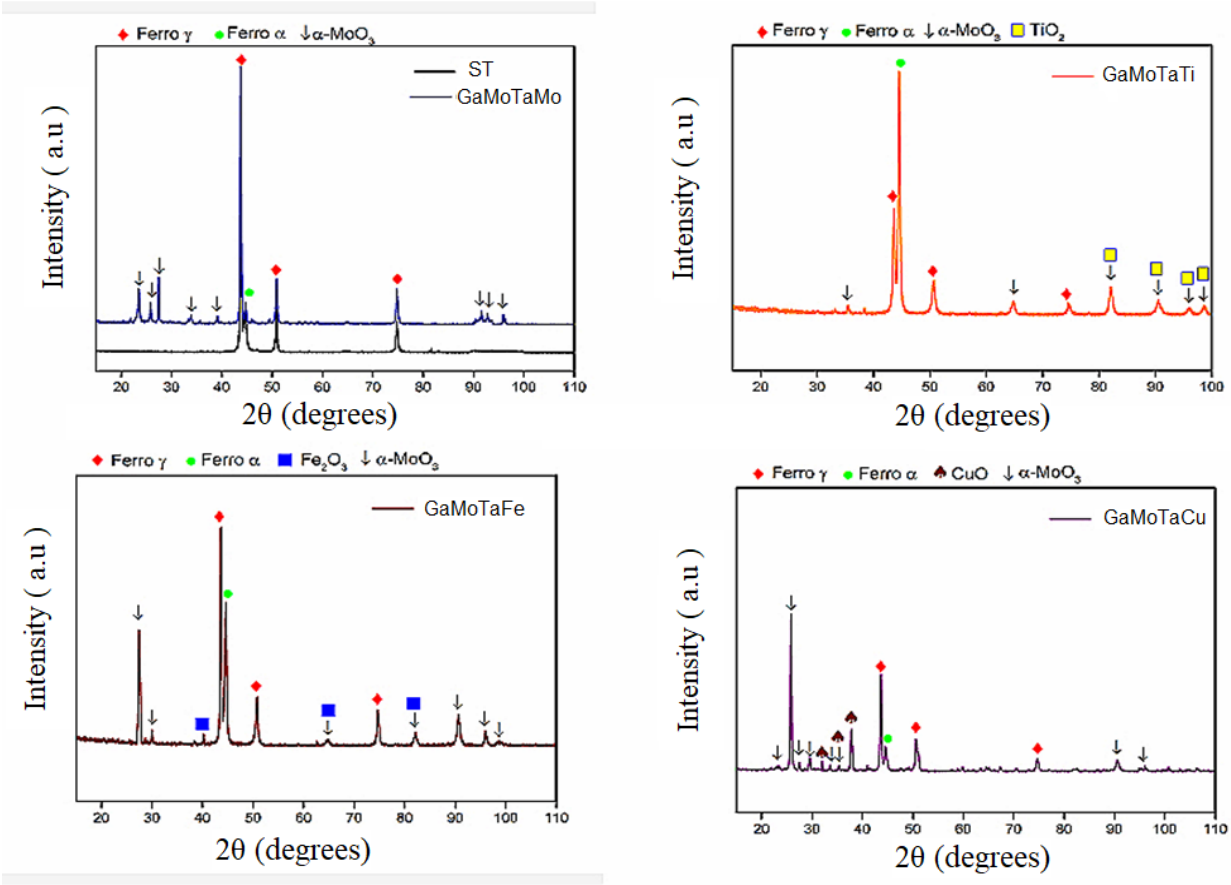

Figure 4 - X-ray diffractograms for AISI 316 steel samples with plasma-deposited film using molybdenum cage with molybdenum (GaMoTaMo), titanium (GaMoTaTi), steel (GaMoTaFe) and copper caps (GaMoTaCu).

The diffractograms reveal the presence of characteristic molybdenum peaks (COD 35076) in all the samples, regardless of the material used for the lids. When analyzing the diffractograms of the samples with titanium, steel and copper lids, the presence of titanium oxide phases is observed,

suggesting that atoms from the lid were incorporated into the formation of the TiO_2 phase. Similarly, the formation of Fe_2O_3 iron oxide (ICSD 1011240) indicates the contribution of both the lid material and the element present in the substrate The formation of copper oxide (COD 9016057) is also observed, which is attributed to the copper lid, as the sample material does not contain copper in its composition. These findings are corroborated by the energy-dispersive spectroscopy (EDS) measurements of samples 2 and 3.

3.2. Vickers Microhardness, Roughness and Adhesion

Figure 5 presents a graph illustrating the average microhardness results of the samples, both untreated and after the treatments. The graph shows the formation of oxide layers, as all the treated samples showed an increase in surface hardness compared to the untreated sample, which had a microhardness of 288.15 HV.

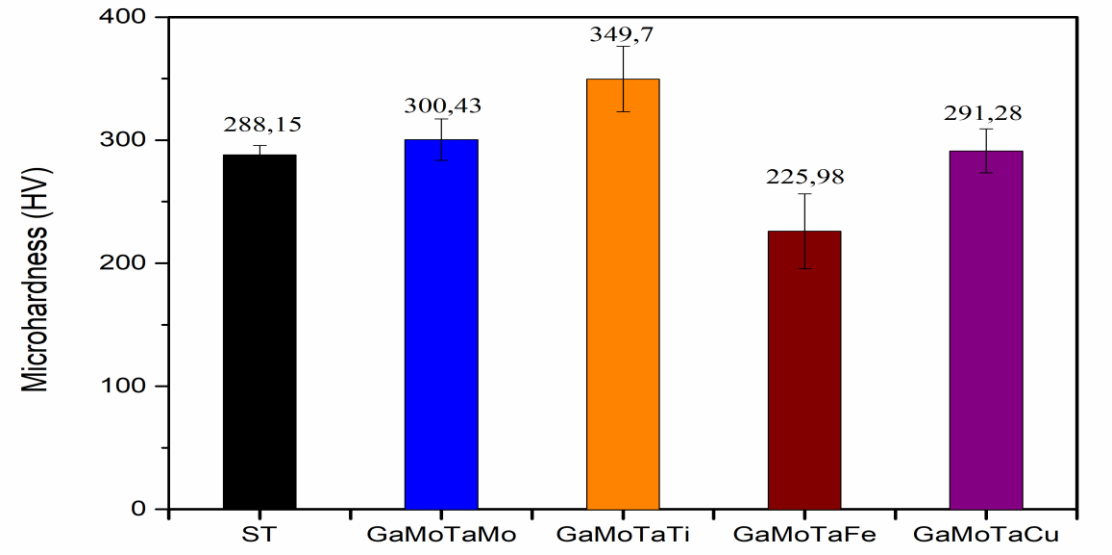

Figure 5 - Microhardness graph

The graph shows that, even under the same conditions, the deposition with the titanium lid exhibited slightly better results compared to the treatments with the other lids. This behavior can be interpreted based on the SEM results, which show a thicker layer on the sample treated with the titanium lid. Additionally, the formation of the TiO_2 phase acts as a barrier to the movement of dislocations, making it difficult to deform the material and contributing to the increase in hardness of the deposited layer [36] [37]. Furthermore, the samples treated with molybdenum and copper lids show a slight increase in microhardness compared to the samples treated with steel lids. This increase may be related to the higher quantity of α-MoO_3 phases, as shown in the diffractograms of the samples, or to the thickness of the layers, which is greater in the samples with molybdenum and copper lids compared to the sample with the steel lid.

Figure 6 presents the results of the surface roughness analyses, showing the numerical values for arithmetic average roughness (Ra) and quadratic average roughness (Rq). The results indicate that plasma deposition had a considerable influence on the surface roughness of the substrate in all the treated samples. In other words, by varying the cage lid while keeping the time and temperature constant for both treatments, an increase in roughness values was detected compared to the untreated sample.

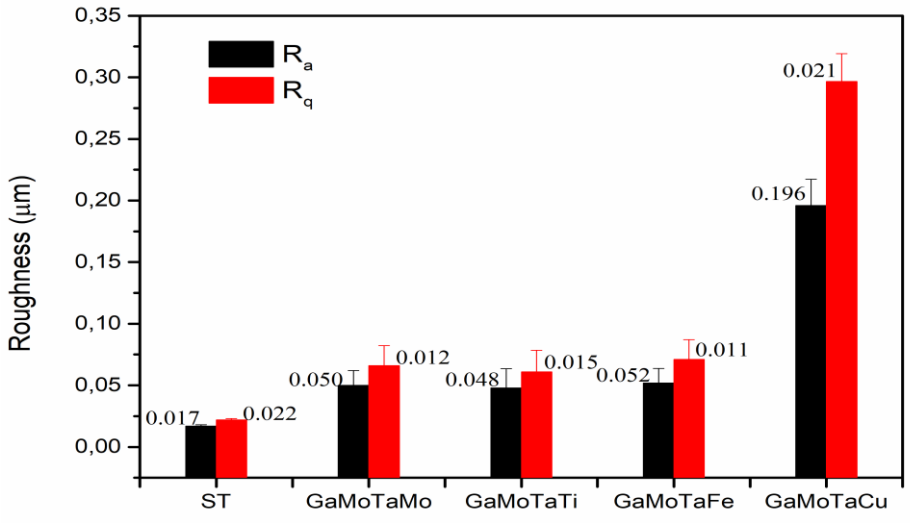

Figure 6 - Roughness measurement

A significant increase in the roughness of the sample with the copper lid was observed. This increase may be related to grain growth caused by the lid material [38]. When analyzed individually, the sample with the titanium lid, which had the greatest layer thickness among the samples evaluated, was the only one to show the lowest roughness values (Ra and Rq). This phenomenon can be attributed to the good adhesion of the film, classified as H1, and the formation of TiO_2 phase, observed in the X-ray diffraction (XRD), which acts as a micro-irregularity filling agent.

In Figure 7, the indentations resulting from the qualitative Daimler-Benz Rockwell-C adhesion test can be observed, applied to samples coated with films using molybdenum cage with molybdenum caps (Figure 6a), titanium (Figure 6b), stainless steel (Figure 6c), and copper (Figure 6d). This test classifies film adhesion into six categories: HF1, HF2, HF3, HF4, HF5, and HF6. Categories HF1 to HF4 indicate good adhesion behavior, while HF5 and HF6 indicate poor adhesion, with visible areas of delamination [39].

All the images show excellent adhesion, classified as HF1. In these images, there are no cracks or regions of detachment. The only mark around the indentations is the accumulation of material at the edges, which suggests a good level of plasticity in the films.

This behavior indicates that the films are classified as HF1, which denotes very good adhesion to the sample, providing durability and resistance to wear in practical applications.

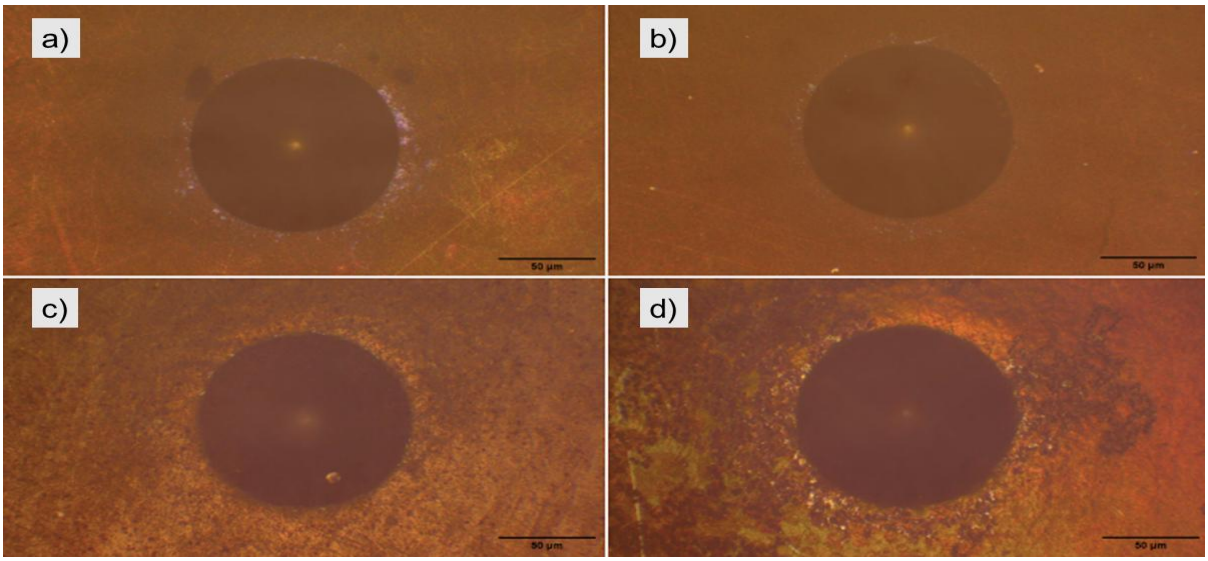

Figure 7 - Adhesion test with Molybdenum cage with Molybdenum, Titanium, Steel and Copper cover.

IV. CONCLUSIONS

Cathodic cage deposition proved to be an efficient technique for obtaining thin metal oxide films with varied properties. By using a molybdenum cage with a titanium lid, it was possible to deposit TiO_2 films with a significant increase in thickness and an improvement in the microhardness of the substrate, indicating potential for applications in areas requiring high resistance to wear.

The use of a molybdenum cage and lid enabled the deposition of MoO_3 films with a homogeneous morphology and crystalline structure, demonstrating the versatility of the technique in obtaining films with specific properties. The inclusion of elements such as iron and copper in the lids, in addition to influencing the composition of the films, altered the thickness of the films and the hardness of the layer.

The results obtained highlight the importance of carefully selecting materials and deposition conditions to obtain films with the desired properties. Cathodic cage deposition opens up new perspectives for surface engineering and the development of functional materials with diverse applications, such as electronic devices, sensors and protective coatings.

ACKNOWLEDGEMENTS

The authors would like to thank LIMAV (Interdisciplinary Laboratory of Advanced Materials) for its support. This study was financed in part by the Coordenação de Aperfeiçoamento de Pessoal de Nível Superior – Brasil (CAPES) – Finance Code 001, and Conselho Nacional de Desenvolvimento Científico e Tecnológico (CNPq)

REFERENCES

[1] P. Srisattayakul, C. Saikaew, A. Wisitsoraat, and D. Phokharatkul, “Reciprocating two-body abrasive wear behavior of DC magnetron sputtered Mo-based coatings on hard-chrome plated AISI 316 stainless steel,” Wear, vol. 378–379, 2017, doi: 10.1016/j.wear.2017.01.005.

[2] M. K. Kazmanli, M. Ürgen, and A. F. Cakir, “Effect of nitrogen pressure, bias voltage and substrate temperature on the phase structure of Mo-N coatings produced by cathodic arc PVD,” Surf Coat Technol, vol. 167, no. 1, pp. 77–82, Apr. 2003, doi: 10.1016/S0257-8972(02)00866-6.

[3] Y. Miyagawa, S. Nakao, K. Baba, M. Ikeyama, K. Saitoh, and S. Miyagawa, “Nitride layers formed by nitrogen implantation into metals,” 1998.

[4] J. Li, D. Xiong, H. Wu, H. Zhu, J. Kong, and R. Tyagi, “Tribological properties of MoN layer on silver-containing nickel-base alloy at high temperatures,” Wear, vol. 271, no. 5–6, pp. 987–993, Jun. 2011, doi: 10.1016/j.wear.2010.12.070.

[5] A. Y. Ganin, L. Kienle, and G. V. Vajenine, “Synthesis and characterisation of hexagonal molybdenum nitrides,” J Solid State Chem, vol. 179, no. 8, pp. 2339–2348, Aug. 2006, doi: 10.1016/j.jssc.2006.05.025.

[6] T. M. Huong, K. Fukushima, H. Ohkita, T. Mizushima, and N. Kakuta, “Design of active molybdenum oxides: β-MoO3 and/or silicomolybdic acid supported on mesoporous MCM-41 catalysts,” Catal Commun, vol. 7, no. 3, pp. 127–131, Mar. 2006, doi: 10.1016/j.catcom.2005.09.007.

[7] M. Naeem et al., “Synthesis of molybdenum oxide on AISI-316 steel using cathodic cage plasma deposition at cathodic and floating potential,” Surf Coat Technol, vol. 406, Jan. 2021, doi: 10.1016/j.surfcoat.2020.126650.

[8] J. L. Falconer and K. A. Magrini-Bair, “Photocatalytic and thermal catalytic oxidation of acetaldehyde on Pt/TiO2,” J Catal, vol. 179, no. 1, 1998, doi: 10.1006/jcat.1998.2215.

[9] S. Corujeira Gallo and H. Dong, “On the fundamental mechanisms of active screen plasma nitriding,” Vacuum, vol. 84, no. 2, pp. 321–325, Sep. 2009, doi: 10.1016/j.vacuum.2009.07.002.

[10] R. R. M. De Sousa et al., “Thin Tin and Tio2film deposition in glass samples by cathodic cage,” Materials Research, vol. 18, no. 2, pp. 347–352, Mar. 2015, doi: 10.1590/1516-1439.313914.

[11] H. F. Moafi, A. F. Shojaie, and M. A. Zanjanchi, "The comparison of photocatalytic activity of synthesized TiO 2 and ZrO 2 nanosize onto wool fibers," Appl Surf Sci, vol. 256, no. 13, pp. 4310–4316, Apr. 2010, doi: 10.1016/j.apsusc.2010.02.022.

[12] T. Iida et al., "TiO2 thin films using organic liquid materials prepared by Hot-Wire CVD method," Thin Solid Films, vol. 516, no. 5, pp. 807–809, Jan. 2008, doi: 10.1016/j.tsf.2007.06.204.

[13] L. Romero, C. Piccirillo, P. M. L. Castro, C. Bowman, M. E. A. Warwick, and R. Binions, "Titanium dioxide thin films deposited by electric field-assisted CVD: Effect on antimicrobial and photocatalytic properties," Chemical Vapor Deposition, vol. 21, no. 1–3, pp. 63–70, Mar. 2015, doi: 10.1002/cvde.201407145.

[14] H. Rasoulnezhad, G. Kavei, K. Ahmadi, and M. R. Rahimipour, "Combined sonochemical/CVD method for preparation of nanostructured carbon-doped TiO 2 thin film," Appl Surf Sci, vol. 408, pp. 1–10, Jun. 2017, doi: 10.1016/j.apsusc.2017.03.014.

[15] D. Manova et al., "Nitrogen incorporation during PVD deposition of TiO2:N thin films," Surf Coat Technol, vol. 312, pp. 61–65, Feb. 2017, doi: 10.1016/j.surfcoat.2016.08.085.

[16] C. J. Tavares et al., "PVD-Grown photocatalytic TiO2 thin films on PVDF substrates for sensors and actuators applications," Thin Solid Films, vol. 517, no. 3, pp. 1161–1166, Dec. 2008, doi: 10.1016/j.tsf.2008.06.024.

[17] M. Yamagishi, S. Kuriki, P. K. Song, and Y. Shigesato, "Thin film TiO2 photocatalyst deposited by reactive magnetron sputtering," in Thin Solid Films, Oct. 2003, pp. 227–231. doi: 10.1016/S0040-6090(03)00987-8.

[18] C. Jayewardena, K. P. Hewaparakrama, D. L. A. Wijewardena, and H. Guruge, "Fabrication of n-Cu2O electrodes with higher energy conversion efficiency in a photoelectrochemical cell," Solar Energy Materials and Solar Cells, vol. 56, no. 1, 1998, doi: 10.1016/S0927-0248(98)00104-4.

[19] S. Ishizuka, S. Kato, T. Maruyama, and K. Akimoto, "Nitrogen Doping into Cu 2 O Thin Films Deposited by Reactive Radio-Frequency Magnetron Sputtering," Jpn J Appl Phys, vol. 40, no. 4S, p. 2765, Apr. 2001, doi: 10.1143/JJAP.40.2765.

[20] K. Nakaoka, J. Ueyama, and K. Ogura, "Photoelectrochemical Behavior of Electrodeposited CuO and Cu[sub 2]O Thin Films on Conducting Substrates," J Electrochem Soc, vol. 151, no. 10, p. C661, 2004, doi: 10.1149/1.1789155.

[21] A. R. Rastkar, A. R. Niknam, and B. Shokri, "Characterization of copper oxide nanolayers deposited by direct current magnetron sputtering," Thin Solid Films, vol. 517, no. 18, pp. 5464–5467, Jul. 2009, doi: 10.1016/j.tsf.2009.01.095.

[22] K. Khojier, H. Savaloni, and Z. Sadeghi, "A comparative investigation on growth, nanostructure and electrical properties of copper oxide thin films as a function of annealing conditions," Journal of Theoretical and Applied Physics, vol. 8, no. 1, Apr. 2014, doi: 10.1007/s40094-014-0116-x.

[23] V. Stranak et al., "Influence of reactive oxygen species during deposition of iron oxide films by high power impulse magnetron sputtering," J Phys D Appl Phys, vol. 51, no. 9, Feb. 2018, doi: 10.1088/1361-6463/aaa9e6.

[24] M. Aronniemi, J. Saino, and J. Lahtinen, "Characterization and gas-sensing behavior of an iron oxide thin film prepared by atomic layer deposition," Thin Solid Films, vol. 516, no. 18, pp. 6110–6115, Jul. 2008, doi: 10.1016/j.tsf.2007.11.011.

[25] G. Wang, Y. Yang, D. Han, and Y. Li, "Oxygen defective metal oxides for energy conversion and storage," Apr. 01, 2017, Elsevier B.V. doi: 10.1016/j.nantod.2017.02.009.

[26] Z. Hubička et al., "Deposition of hematite Fe2O3 thin film by DC pulsed magnetron and DC pulsed hollow cathode sputtering system," Thin Solid Films, vol. 549, pp. 184–191, Dec. 2013, doi: 10.1016/j.tsf.2013.09.031.

[27] C. X. Kronawitter, S. S. Mao, and B. R. Antoun, "Doped, porous iron oxide films and their optical functions and anodic photocurrents for solar water splitting," Appl Phys Lett, vol. 98, no. 9, Feb. 2011, doi: 10.1063/1.3552711.

[28] G. Zotti, G. Schiavon, S. Zecchin, and U. Casellato, "Electrodeposition of Amorphous Fe2 O 3 Films by Reduction of Iron Perchlorate in Acetonitrile," J Electrochem Soc, vol. 145, no. 2, pp. 385–389, Feb. 1998, doi: 10.1149/1.1838273.

[29] N. Özer and F. Tepehan, "Optical and electrochemical characteristics of sol–gel deposited iron oxide films," Solar Energy Materials and Solar Cells, vol. 56, no. 2, pp. 141–152, Jan. 1999, doi: 10.1016/S0927-0248(98)00152-4.

[30] M. Gartner, M. Crisan, A. Jitianu, and R. Scurtu, "Spectroellipsometric Characterization of Multilayer Sol-Gel Fe 2 O 3 Films," 2003.

[31] S. Mathur et al., "Nanostructured films of iron, tin and titanium oxides by chemical vapor deposition," Thin Solid Films, vol. 502, no. 1–2, pp. 88–93, Apr. 2006, doi: 10.1016/j.tsf.2005.07.249.

[32] M. Naeem, M. Shafiq, M. Zaka-ul-Islam, N. Nawaz, J. C. Díaz-Guillén, and M. Zakaullah, "Effect of cathodic cage size on plasma nitriding of AISI 304 steel," Oct. 15, 2016, Elsevier B.V. doi: 10.1016/j.matlet.2016.05.144.

[33] E. A. M. Filho et al., "Microstructure, mechanical, and tribological properties of transition metal (Nb, V, W) nitride coating on AISI-1045 steel by cathodic cage plasma deposition," Journal of Vacuum Science & Technology A, vol. 42, no. 5, Sep. 2024, doi: 10.1116/6.0003773/3305678.

[34] R. R. M. De Sousa, F. O. De Araújo, K. J. B. Ribeiro, J. A. P. Da Costa, R. S. De Sousa, and C. Alves, "Uniformity of temperature in cathodic cage technique in nitriding of austenitic stainless steel AISI 316," https://doi.org/10.1179/174329408X326830, vol. 24, no. 4, pp. 313–318, Jul. 2008, doi: 10.1179/174329408X326830.

[35] A. B. V. Leitao et al., "Novel synthesis of molybdenum nitride/oxide on AISI-316 steel assisted with active screen plasma treatment," Mater Res Express, vol. 6, no. 11, Sep. 2019, doi: 10.1088/2053-1591/ab42e1.

[36] H. M. Mahan, S. V. Konovalov, K. Osintsev, and I. Panchenko, "THE INFLUENCE OF TiO2 NANOPARTICLES ON THE MECHANICAL PROPERTIES AND MICROSTRUCTURE OF AA2024 ALUMINIUM ALLOY," Materiali in Tehnologije, vol. 57, no. 4, pp. 379–384, 2023, doi: 10.17222/mit.2023.898.

[37] K. Aniołek, A. Barylski, and M. Kupka, "Friction and wear of oxide scale obtained on pure titanium after high-temperature oxidation," Materials, vol. 14, no. 13, Jul. 2021, doi: 10.3390/ma14133764.

[38] D. S. C. Halin, I. A. Talib, A. R. Daud, and M. A. A. Hamid, "Cu2O thin film for photoelectrochemical solar cell (PESC) of ITO/Cu2O/PVC-LiClO4/graphite," in AIP Conference Proceedings, American Institute of Physics Inc., Apr. 2017. doi: 10.1063/1.4981845.

[39] N. Vidakis, A. Antoniadis, and N. Bilalis, "The VDI 3198 indentation test evaluation of a reliable qualitative control for layered compounds," in Journal of Materials Processing Technology, Dec. 2003, pp. 481–485. doi: 10.1016/S0924-0136(03)00300-5.